Vol 15 No 7, July 2006
1009-1963/2006/15(07)/1492-05

Chinese Physics

© 2006 Chin. Phys. Soc.
and IOP Publishing Ltd

An ingenious approach of determining hydrogen isotope solubilities, diffusivities and permeabilities in GWHER-1 stainless steel*

Chen Zhi(陈 志)[a)†], Deng Bai-Quan(邓柏权)[a)], Peng Li-Lin(彭利林)[a)], Feng Kai-Ming(冯开明)[a)], Du Jia-Ju(杜家驹)[b)], and Mao Ou(毛 鸥)[b)]

[a)] *Southwestern Institute of Physics, Chengdu* 610041, *China*

[b)] *Institute of Solid State Physics, Chinese Academy of Sciences, Hefei* 230031, *China*

(Received 30 September 2005; revised manuscript received 28 November 2005)

In this paper, by using an ingenious method, the hydrogen isotope solubilities and diffusivities in GWHER-1 stainless steel have been determined by a vacuum heating degassing approach at the temperature range of 597–1022 K on a set of specimens with different sizes previously charged for 24 h under a hydrogen isotope pressure of 10^5 Pa in the temperature range of 800–1000 K. The permeabilities are then derived from the relation $\Phi = DK_s$. It is found $D = 1.52\times10^{-6}\exp(-54100/RT)$, $K_s = 2.2\times10^{-6}\exp(-5400/RT)$ and $\Phi = 3.3\times10^{-12}\exp(-59500/RT)$ for hydrogen, where K_s (Sieverts' constant) is given in $Pa^{-1/2}$, D in $m^2\cdot s^{-1}\cdot Pa^{-1/2}$, T in K and R=8.31J·mol^{-1}·K^{-1}. By taking isotope effects into account, the corresponding Arrhenius relations for deuterium and tritium are also deduced.

Keywords: hydrogen isotope, vacuum heating degassing, GWHER-1 stainless steel, transport properties

PACC: 2852F, 5120, 8640K

1. Introduction

The total demanded tritium inventory is one of the most important key issues of the utmost concern for initiating a fusion reactor in the future. Moreover, the neutral hydrogen isotopes released from the plasma facing component materials and their retention in blanket structural materials have notable impacts on either neutral particle transport, recycling in the edge plasma, and density profile control during discharge in present devices, or tritium extraction and recovery in future tokamak reactors. To predict the total tritium inventory for starting up a fusion reactor and the tritium distribution in all components of reactor system, the hydrogen isotope solubilities, diffusivities and permeabilities are urgently required. The experimental investigations of hydrogen isotope diffusivities and solubilities in GWHER-1 steel (Hydrogen-Embrittlement-Resistant stainless steel made by China-Great-Wall-Steel-Mill) have been performed.

Our previous work[1] was aimed at the experimental studies of electrochemical hydrogen permeation in GWHER-1 steel and the measurement of H_2 released. We obtained the characteristic temperature of peak outgassing and the binding energy of some kinds of hydrogen traps in GWHER-1 material. An ingenious approach for determination of the hydrogen and its isotope solubilities and diffusivities in a set of various size samples of GWHER-1 steel is highlighted in this paper. The approach[2] used in this investigation is based on the measurement of hydrogen isotope amount released within a time interval Δt during vacuum heating degassing of a metallic sample which was previously charged at hydrogen isotope partial pressure 10^5 Pa (i.e. 1 atm) in the temperature range of 800–1000 K for 24 h and then was quickly lowered into liquid nitrogen quenching bath, as a result, the hydrogen isotopes are frozen in the sample as the same condition as those at the end of charging. Based on the solutions derived from diffusion equations, the solubility coefficients K_s and diffusivities D can be determined by a nonlinear least-squares fitting of the experimental data. The permeability coefficients are

*Project supported by the National Natural Science Foundation of China (Grant No 10275017).

†E-mail: chenz@swip.ac.cn

obtained by using the relationship $\Phi = DK_s$.[3]

2. Physical background

Firstly, a GWHER-1 cylinder of radius r_0= 10 mm, length l=10 mm is considered and hydrogen is used as charged gas. The nonlinear effects and surface chemical processes are not involved so that the diffusion coefficient of the specimen is independent of the hydrogen concentration. When hydrogen has been charged, the process of hydrogen degassing in vacuum can be described by[4]

$$\frac{\partial C}{\partial t} = D\left[\frac{1}{\rho}\frac{\partial}{\partial \rho}\left(\rho\frac{\partial C}{\partial \rho}\right) + \frac{1}{\rho^2}\frac{\partial^2 C}{\partial \varphi^2} + \frac{\partial^2 C}{\partial z^2}\right], \quad (1)$$

where ρ, φ, z are variables of cylindrical coordinates, $C(\rho, z, t)$ is the hydrogen concentration in the specimen and D is the diffusion coefficient. The boundary conditions are taken as

$$C(r_0, z, t) = C(\rho, 0, t) = C(\rho, l, t) = 0, \quad (2)$$

the initial condition

$$C(\rho, z, 0) = C_0 \quad (\rho \le r_0, 0 \le z \le l). \quad (3)$$

The solution of Eqs.(1), (2) and (3) should be

$$C(\rho, z, t) = \sum_{i,n=1}^{\infty} \frac{4C_0(1-\cos n\pi)}{n\pi\mu_i J_1(\mu_i)} J_0\left(\frac{\mu_i}{r_0}\rho\right) \times \sin\left(\frac{n\pi z}{l}\right)\exp\left(-k_{ni}^2 Dt\right), \quad (4)$$

where

$$k_{ni}^2 = \frac{\mu_i^2}{r_0^2} + \frac{n^2\pi^2}{l^2} \quad (5)$$

and μ_i is the ith root of first order Bessel's function.

For linearly uniform heating of the sample in vacuum, the diffusion coefficient D is time-dependent, which is equal to

$$D(t) = D_0 \exp\left[\frac{-H}{kT(t)}\right], \quad (6)$$

here k is Boltzmann's constant, and

$$T(t) = T_0 + \theta t, \quad (7)$$

where θ= constant, which is the temperature-rising rate due to heating. Assuming that Fick's law is valid at any time, from the mass conservation relation we know that the decrease of hydrogen content in the sample is equal to the amount released within the interval from t to $t + \Delta t_i$

$$Q(t, t+\Delta t_i) = \sum_{i,n=1}^{\infty} \frac{8C_0\pi r_0^2 l(1-\cos n\pi)^2}{(n\pi)^2\mu_i^2}\left[\exp\left(-k_{n,i}^2\int_0^t D(t')\,\mathrm{d}t'\right) - \exp\left(-k_{n,i}^2\int_0^{t+\Delta t_i} D(t')\,\mathrm{d}t'\right)\right]. \quad (8)$$

where k_{ni} is given by Eq.(5). Q is measured by experiment and the relationship can be obtained by a nonlinear least-squares fit to the experimental data.

Secondly, geometry of GWHER-1 stainless steel specimen considered is a big disc 0.5 mm×20.3 mm, which was previously charged under a H_2 pressure of 10^5 Pa at a temperature of 1000 K for a long time. It can be regarded as a one-dimensional problem in slab geometry because the thickness 0.5 is much smaller than the diameter 20.3 mm.

Thirdly, sample geometry considered is a long rectangular parallelepiped 12.58 mm×12.5 mm× 1.52 mm. It has been treated as a two-dimensional problem.

3. Experimental arrangement

Three different geometries of GWHER-1 specimens described above have been investigated. The detailed composition of GWHER-1 steel was published previously.[5] They were first charged under the same hydrogen pressure of 10^5 Pa at a fixed temperature of 1000K for disc and long rectangular parallelepiped specimens and at 800K for the cylinder geometry. After charging for a long enough time, the specimens were immediately lowered into a liquid-nitrogen-quenching bath (LN_2) in order to maintain hydrogen concentration and its profiles in the same conditions as those at the end moment of charging. The hydrogen-charging furnace with an attached liquid quenching bath is illustrated in Fig.1.

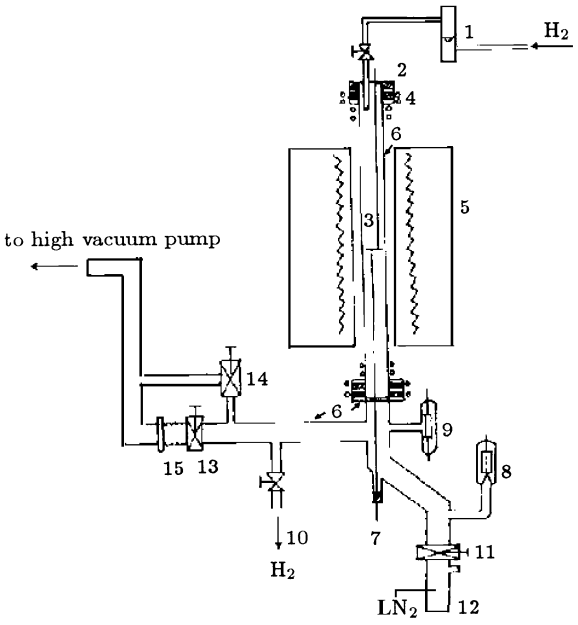


Fig.1. Schematic view of the hydrogen charging furnace with an attached liquid nitrogen quenching bath. (1) Rotor flowmeter, (2) vacuum tight cap, (3) sample supporter, (4) cooling water jacket, (5) upright furnace, (6) stainless steel (s.s.) vacuum pipe and junction, (7) thermocouple, (8) gauge, (9) low vacuum gauge, (10) H_2 outlet (pressure $\geq$1atm), (11) high vacuum gate valve, (12) LN_2 quenching bath, (13) vacuum main valve, (14) bypass vacuum adjusting valve, (15) metal bellow.

For different sample geometries, the required times for hydrogen charging are different. They should be long enough to make the H_2 concentration inhomogeneity in the sample less than the required one. Since the longer charged time is, the less H_2 concentration inhomogeneity will be. For a given demanded uniformity of 1%, the necessary minimum times for hydrogen charging can be determined and the charging times depend on the demanded inhomogeneity, geometries, and diffusivity. In our cases, the minimum charging times are 11 s and 7×10^4 s for the disc and cylinder respectively.

4. Demanded inhomogeneity and charging time setting

Suppose the initial hydrogen concentration is zero, i.e. $\tilde{C}(\rho, z, 0) = 0$, and the volume of the sample is much smaller than the charging chamber. The hydrogen thermodynamic balance is kept on the sample surface during hydrogen charging, i.e. the hydrogen concentration remains constant on the surface:

$$\tilde{C}(\rho = r_0, z = 0, l, t) = C_0. \tag{9}$$

Let

$$\tilde{C}(\rho, z, t) = \tilde{C}_1(\rho, z, t) + C_0, \tag{10}$$

then we have initial and boundary conditions

$$\begin{aligned} &\tilde{C}_1(\rho, z, t = 0) = -C_0, \\ &\tilde{C}_1(\rho, z, t) = 0 \quad (\text{at} \quad \rho = r_0 \text{ and } z = 0, l). \end{aligned} \tag{11}$$

By solving the diffusion equation, we get

$$\tilde{C}_1(\rho, z, t) = -C(\rho, z, t), \tag{12}$$

where $C(\rho, z, t)$ is given by Eq.(4), therefore

$$\tilde{C}(\rho, z, t) = C_0 - C(\rho, z, t). \tag{13}$$

The inhomogeneity of hydrogen absorption within the cylinder specimen can be expressed as

$$\tilde{\delta}(\rho, z, t) = \left[C_0 - \tilde{C}(\rho, z, t)\right]/C_0 = C(\rho, z, t)/C_0 \tag{14}$$

and $\tilde{\delta}(\rho, z, t)$ will take its maximum at $\rho = 0, z = l/2$, it means

$$\begin{aligned} \tilde{\delta}(0, l/2, t) =& C(0, l/2, t)/C_0 \\ =& \sum_{i=1,n=1}^{\infty} \frac{4}{n\pi}(1 - \cos(n\pi)) \\ & \times \frac{\sin\left(\frac{n\pi}{2}\right)}{\mu_i J_1(\mu_i)} \exp\left(-k_{ni}^2 Dt\right) \\ \cong& \frac{8}{\pi\mu_1 J_1(\mu_1)} \exp(-k^2 Dt), \end{aligned} \tag{15}$$

where k^2 is given by

$$k^2 = \frac{\pi^2}{l^2} + \frac{\mu_1^2}{r_0^2}. \tag{16}$$

If 1% inhomogeneity is demanded, then the charging time condition

$$k^2 Dt \geq 5.3 \tag{17}$$

should be met for cylinder sample. For other two geometries of specimens, the similar charge time conditions can be derived by the same method as above.

5. Degassing and data fitting

The apparatus for vacuum hydrogen degassing and measurement of released hydrogen is shown schematically in Fig.2. After hydrogen charging and being frozen by LN_2, the specimen is put into the quartz vacuum chamber which has been heated to the

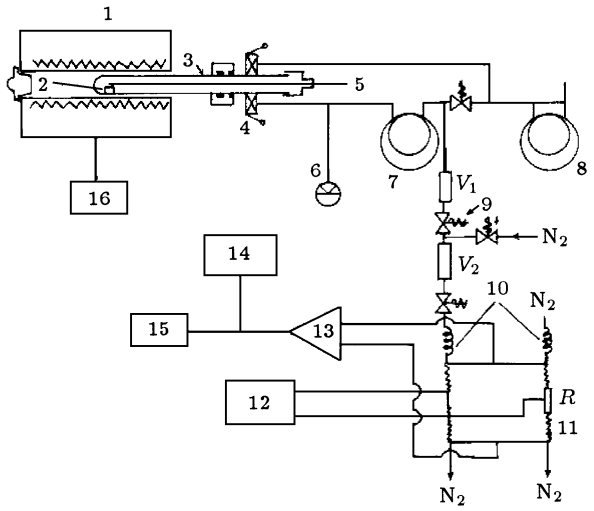


Fig.2. Experimental configuration for hydrogen release by heating in vacuum. (1) Resistance furnace, (2) sample, (3) quartz vacuum chamber, (4) manual surface-sealed valve, (5)thermocouple, (6)vacuum gauge, (7) collecting pump, (8) mechanical pump, (9) electromagnetic valve, (10) chromatogram column, (11) thermoconductive pool, (12) regulated DC power, (13) preamplifier, (14) recorder, (15) integrator amplifier, (16) programmed temperature controller.

set temperature. When the specimen reaches this temperature we start timing and, set t=0. The hydrogen released from the specimen is collected in chamber V_2. At time t, within a time interval Δt, the quantity of hydrogen collected in V_2 is determined by flushing it into the chromatogram. We let the quantity of hydrogen be equal to $Q(t_i) = y_i$, and obtain a dataset $(y_i, t_i, \Delta t_i)$ which can be fitted as a function $Q(\alpha, t, \Delta t)$, where $\alpha = (\alpha_1, \alpha_2, \alpha_3, \ldots, \alpha_l)$ are fitting parameters and $(t, \Delta t)$ are variables. Using nonlinear regression analysis, we can find $\alpha^* = (\alpha_1^*, \alpha_2^*, \alpha_3^*, \ldots, \alpha_l^*)$ where $F(\alpha^*)$ is a minimum, at which $F(\alpha)$ is

$$F(\alpha) = \sum_{i=1}^{m} [y_i - Q(\alpha, t_i, \Delta t_i)]^2. \qquad (18)$$

6. Results and discussion

Figure 3 shows the $Q(t)$ curves for two different sample geometries and different set temperatures when t=300s. The solid lines are the curves from nonlinear least-squares fitting. The diffusivity D and initial hydrogen concentration C_0 are listed in Table 1. Figure 4 shows the diffusivity as a function of the reciprocal temperature T^{-1}, that is ln$D$ versus T^{-1}. Figure 5 shows the variation of hydrogen solubility S_{H} with the reciprocal temperature for hydrogen charging. The data at charging temperature of 1300K are not included in Table 1 because of vacuum failure at this high temperature. The solubility data exhibit some fluctuations. This is due to a limitation of the experimental technique which does not discriminate between hydrogen released from the normal lattice and from that in the defects or traps. Therefore, a different total amount of released hydrogen will be obtained at different degassing temperatures.

Table 1. Experimental conditions and fitting parameters for different specimen geometries.

Specimen geometries /mm	H_2 charging pressure /Pa	H_2 charging temperature /K	degassing temperature /K	fitting parameters D /(m^2/s)	C_0 /ppm[H_2]
0.5×Φ20.3	10^5	1000	597.5	2.79×10^{-11}	2.6
12.58×12.5×1.52	10^5	1000	764.5	3.6×10^{-10}	7.7
10×Φ10	10^5	800	1022	2.59×10^{-9}	7.9

Compared with the more standard permeation method, our degassing technique has the advantages that any geometry of specimen can be used in the degassing method. It is suitable for a wide temperature range and has no vacuum leakage problems, so that diffusivity at higher temperatures can be measured.

Regression analysis of our experimental data yields Arrhenius relations for H_2

$$D = 1.52 \times 10^{-6} \exp\left(\frac{-54100}{RT}\right) \quad \left(\mathrm{m^2/s}\right), \qquad (19)$$

$$K_{\mathrm{s}} = 2.2 \times 10^{-6} \exp\left(\frac{-5400}{RT}\right) \quad \left(\mathrm{Pa^{-1/2}}\right), \qquad (20)$$

$$\Phi = 3.3\times10^{-12} \exp\left(\frac{-59500}{RT}\right) \quad \left(\mathrm{m^2/s}\right) \mathrm{Pa^{-1/2}}, \qquad (21)$$

with the unit of temperature in K and R=8.31J·mole^{-1}·K^{-1}. These results are in fair agreement with the results of other authors for similar material 316L steel.[6]

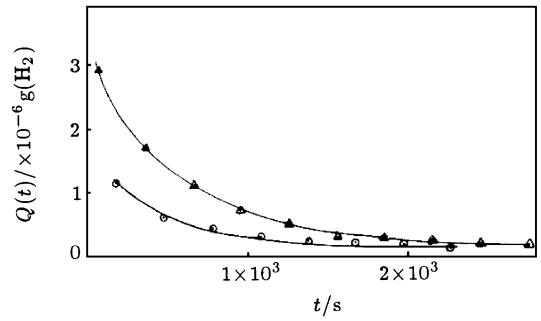


Fig.3. Experimental measurements and fitting curves for hydrogen release at fixed temperature in vacuum. For points represented by △, T=764.5K, sample thickness δ=1.52mm; for points represented by ○, T=597.5 K, sample thickness δ=0.5mm; for curves represented by continuous lines —computer fitting curves.

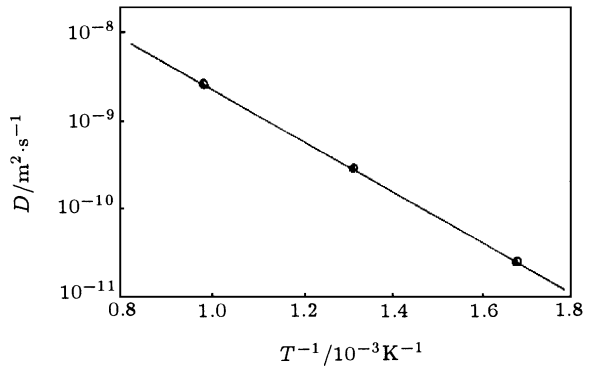


Fig.4. Variation of diffusivity ln$D$ with reciprocal temperature.

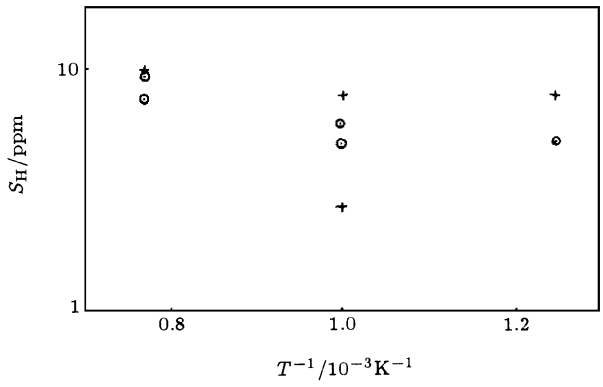


Fig.5. Variation of solubility S_H with reciprocal temperature.

7. Isotope effect extrapolation

The hydrogen isotope permeabilities in material are governed by the observed activation energy E_H, E_D, E_T and can be expressed as

$$\Phi_\mathrm{H} \propto K_\mathrm{H}\exp\left(-\frac{E_\mathrm{H}}{RT}\right), \tag{22}$$

$$\Phi_\mathrm{D} \propto K_\mathrm{D}\exp\left(-\frac{E_\mathrm{D}}{RT}\right), \tag{23}$$

$$\Phi_\mathrm{T} \propto K_\mathrm{T}\exp\left(-\frac{E_\mathrm{T}}{RT}\right), \tag{24}$$

where the K_H, K_D, K_T are permeation constants.

Taking isotope effects into account,[7] we can obtain a set of similar Arrhenius relations for D_2 and T_2. For deuterium we got

$$D = 1.52\times10^{-6}\exp\left(\frac{-54100}{RT}\right) \quad \left(\mathrm{m^2/s}\right), \tag{25}$$

$$K_\mathrm{s} = 3.06\times10^{-6}\exp\left(\frac{-4880}{RT}\right) \quad \left(\mathrm{Pa^{-1/2}}\right), \tag{26}$$

$$\Phi = 4.65\times10^{-12}\exp\left(\frac{-58980}{RT}\right) \quad \left(\mathrm{m^2/s}\right)\cdot\mathrm{Pa^{-1/2}}, \tag{27}$$

and for T_2

$$D = 9.38\times10^{-6}\exp\left(\frac{-74910}{RT}\right) \quad \left(\mathrm{m^2/s}\right), \tag{28}$$

$$K_\mathrm{s} = 4.06\times10^{-6}\exp\left(\frac{-4400}{RT}\right) \quad \left(\mathrm{Pa^{-1/2}}\right), \tag{29}$$

$$\Phi = 3.81\times10^{-11}\exp\left(\frac{-79310}{RT}\right) \quad \left(\mathrm{m^2/s}\right)\cdot\mathrm{Pa^{-1/2}}, \tag{30}$$

respectively. Tritium retention and permeation in plasma facing components made of GWHER-1s.s. might be a potential problem in the future. Experiments for studying hydrogen behaviour in GWHER-1s.s. with various coated films have been performed.

References

[1] Deng B Q and Huang Q R 1990 *SWIP Ann. Rep.* **52**
[2] Grant D M, Cumming D L and Blackburn D A 1988 *J. Nucl. Mater.* **152** 139
[3] Hu L H, Dai S Y and Wang K J 2003 *Acta Phys. Sin.* **52** 2135 (in Chinese)
[4] Zeng L Y, Dai S Y, Wang K J, Shi C W, Kong F T, Hu L H and Pan X 2005 *Acta Phys. Sin.* **54** 53 (in Chinese)
[5] Qian J P, Sun J G and Xu Z Y 1989 *Fusion Eng. Des.* **9** 135
[6] Reiter F, Camposilvan J, Caorlin M, Saibene G and Sartori R 1985 *Fusion Technol.* **8** 2344
[7] Hickman R G 1974 *Technology of Controlled Thermonuclear Fusion Experiments and the Engineering Aspects of Fusion Reactors.* (United States Atomic Energy Commission: Technical Information Center, Office of Information Services) p105